Supporting Information

Ethanol dehydrogenation to acetaldehyde over Co@N-doped carbon

Aleksey N. Chernov, Tatiana V. Astrakova, Konstantin Yu. Koltunov, Vladimir I. Sobolev*

*visobo@catalysis.ru

Table of contents

Catalysts characterization techniques

1. Brunauer–Emmett–Teller (BET) specific surface area

The porous structure parameters were determined from N_2 adsorption isotherms at 77 K on ASAP-2400 (Micromeritics, USA) analyzer after degassing the samples at 150 °C to a residual pressure of 30 mTorr (4 Pa). The total accessible surface area by the BET method, and the total volume of pores with effective sizes up to 100–200 nm (V_{total}) were estimated from the amount of adsorption at the relative nitrogen pressure of ~ 0.99. A micropore volume and surface areas of mesopores and micropores were calculated by the standard software provided by the instrument.

2. Powder X-ray diffraction

A powder X-ray diffraction (XRD) analysis was performed on a Siemens D500 instrument with CuKα radiation and θ–2θ focusing geometry. The instrument was equipped with a graphite monochromator in the reflected beam, which made it possible to diminish the contribution from the cobalt fluorescence under the copper radiation. A scintillation detector was used for signal detection. Measurements were made in the scanning mode at 2θ angles in the 10–70° range at a step of 0.05° and accumulation duration at a point of 3 s. The analysis was made with a Bruker EVA software package contained in the hardware-software complex. The X-ray diffraction patterns were interpreted by the aid of the ICDD (International Center for Diffraction Data) PDF-2 database.

3. High-resolution transmission electron microscopy (HRTEM)

Micrographs were obtained with JEM-2010 (JEOL, Japan) instrument with lattice resolution 0.14 nm and accelerating voltage 200 kV. The samples were prepared by ultrasonic dispersing in ethanol and consequent deposition of the suspension upon a "holey" carbon film supported on a copper grid. Local elemental analysis was performed with the energy dispersive X-ray (EDX) method on «QUANTAX 200-TEM» spectrometer (Bruker, Germany) equipped with XFLASH detector with energy resolution ~ 130 eV.

4. HRTEM and scanning transmission electron microscopy (STEM)

HRTEM and STEM images were obtained with ThemisZ (Thermo Fisher Scientific, USA) instrument with lattice resolution of 0.07 nm and accelerating voltage 200 kV. The samples were prepared by ultrasonic dispersing in ethanol and consequent deposition of the suspension upon a "holey" carbon film supported on a copper grid. Local elemental
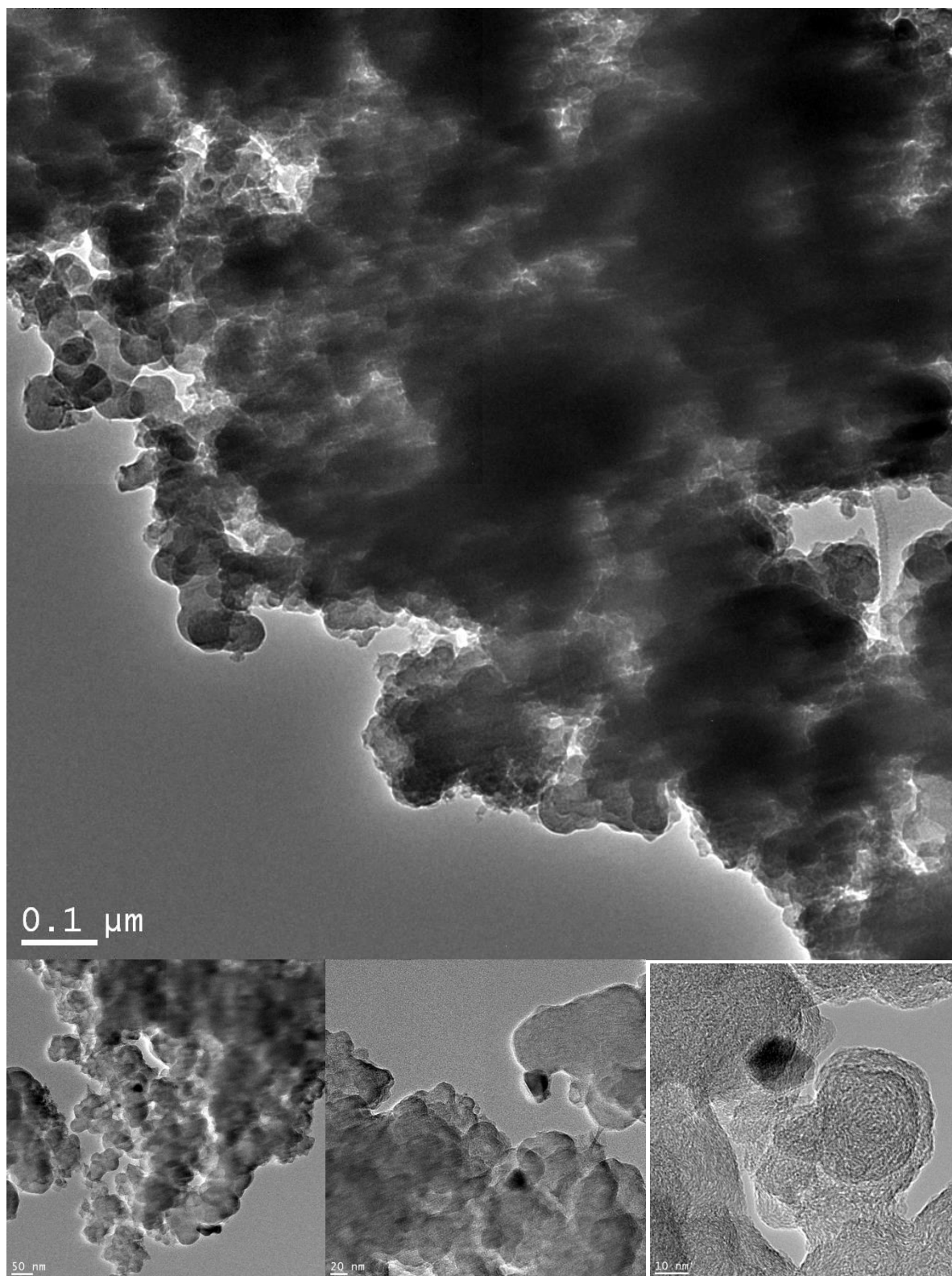
analysis was performed with the energy dispersive X-ray (EDX) method on ThemisZ (Thermo Fisher Scientific, USA) spectrometer equipped with Si-detector with energy resolution 128 eV.
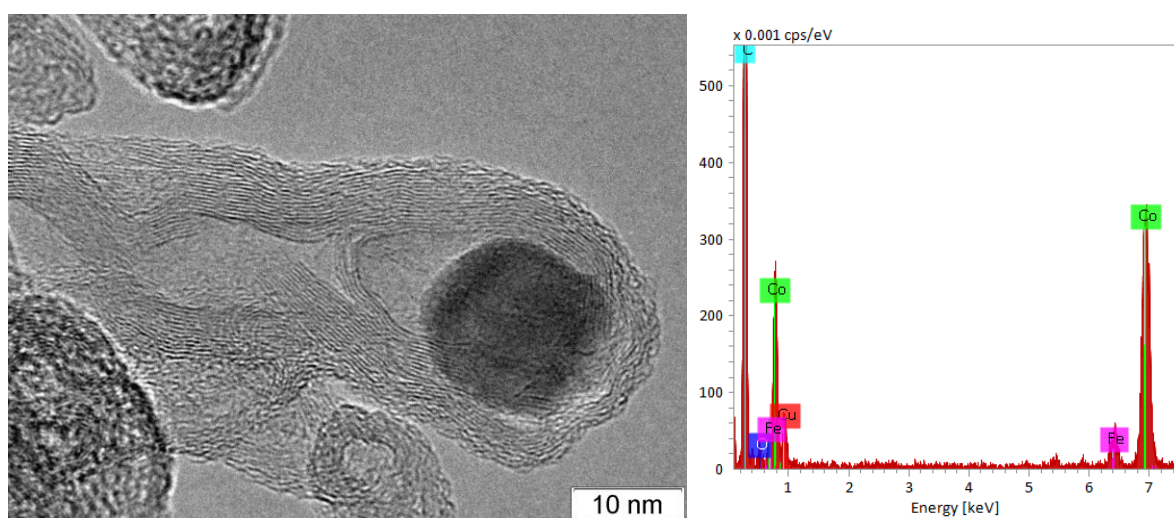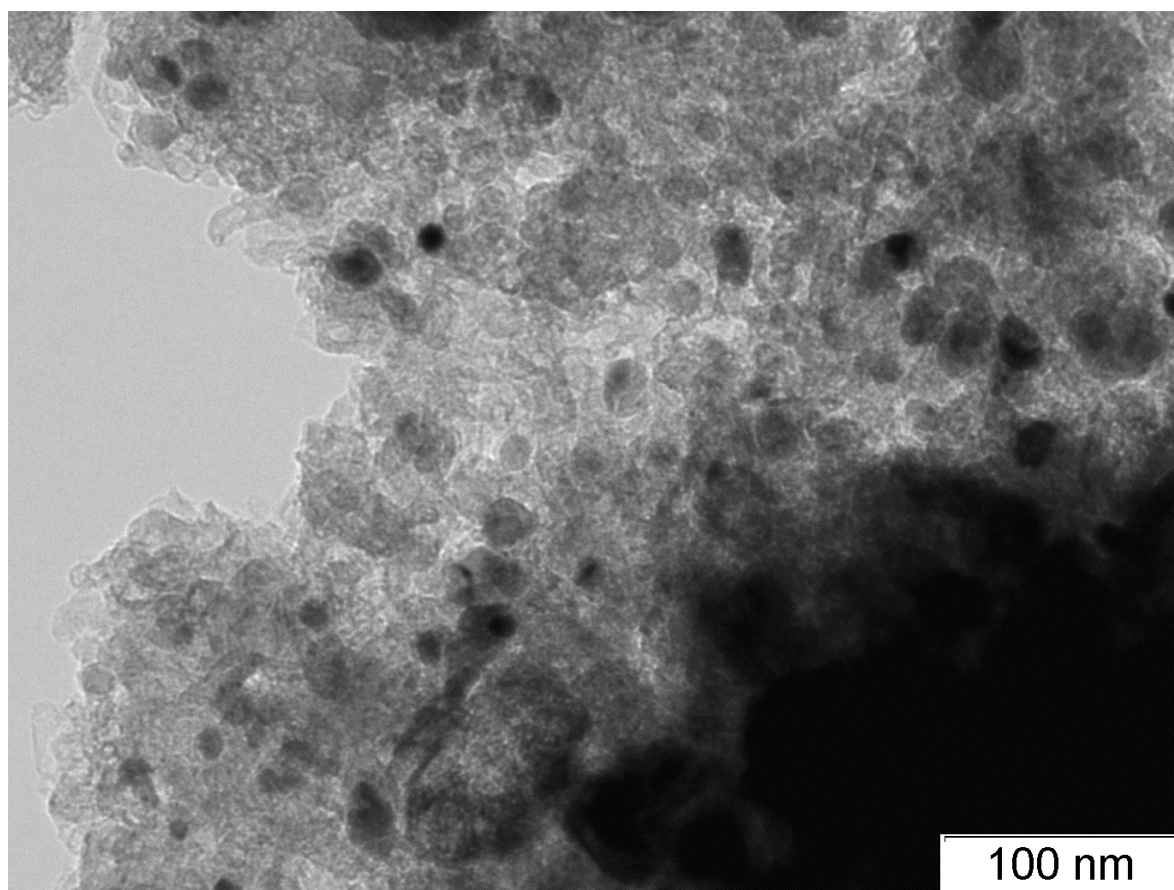
5. X-ray fluorescence (XRF)

The content of Co element in the samples was measured by XRF using a sequential spectrometer ARL Perform'X with a Rh anode X-ray tube.

6. X-ray photoelectron spectroscopy (XPS)

X-ray photoelectron spectra were recorded on a SPECS (Germany) photoelectron spectrometer using a hemispherical PHOIBOS-150-MCD-9 analyzer (Al K_α radiation, hν = 1486.6 eV, 150 W). The binding energy (BE) scale was pre-calibrated using the positions of the peaks of Au $4f_{7/2}$ (BE = 84.0 eV) and Cu $2p_{3/2}$ (BE = 932.67 eV) core levels. The binding energy value of peaks was corrected to consider the sample charging by referencing to the C 1s (284.5 eV, internal standard). The sample in the form of powder was loaded onto a conducting double-sided copper scotch. The survey spectrum and the narrow spectra (C 1s, N 1s, O 1s and Co 2p) were registered at the analyzer pass energy of 20 eV. Atomic ratios of the elements were calculated from the integral photoelectron peak intensities, which were corrected by corresponding sensitivity factors based on Scofield photoionization cross-sections. Analysis of the data was carried out by the software of XPS Peak 4.1 provided by the instrument.
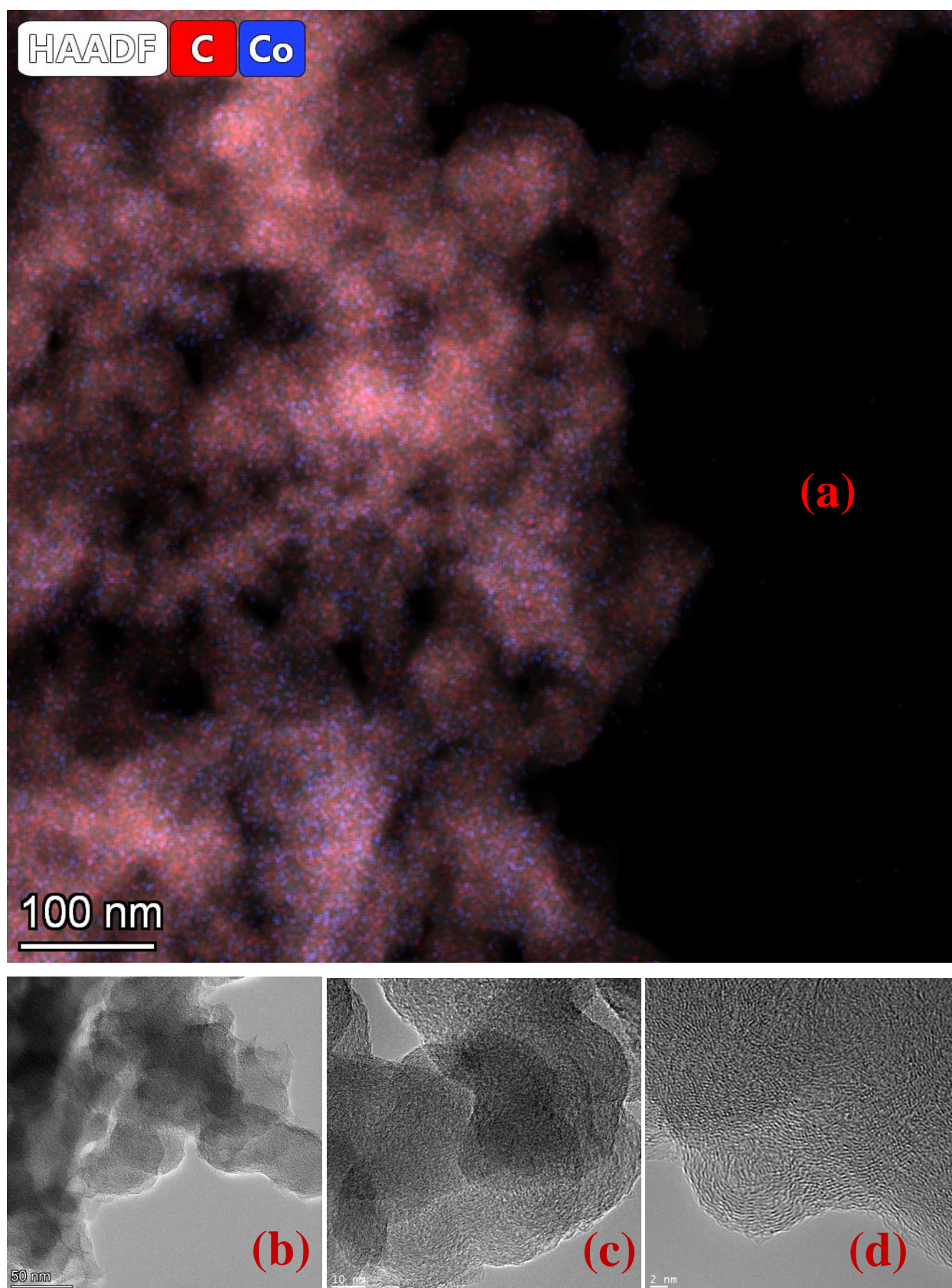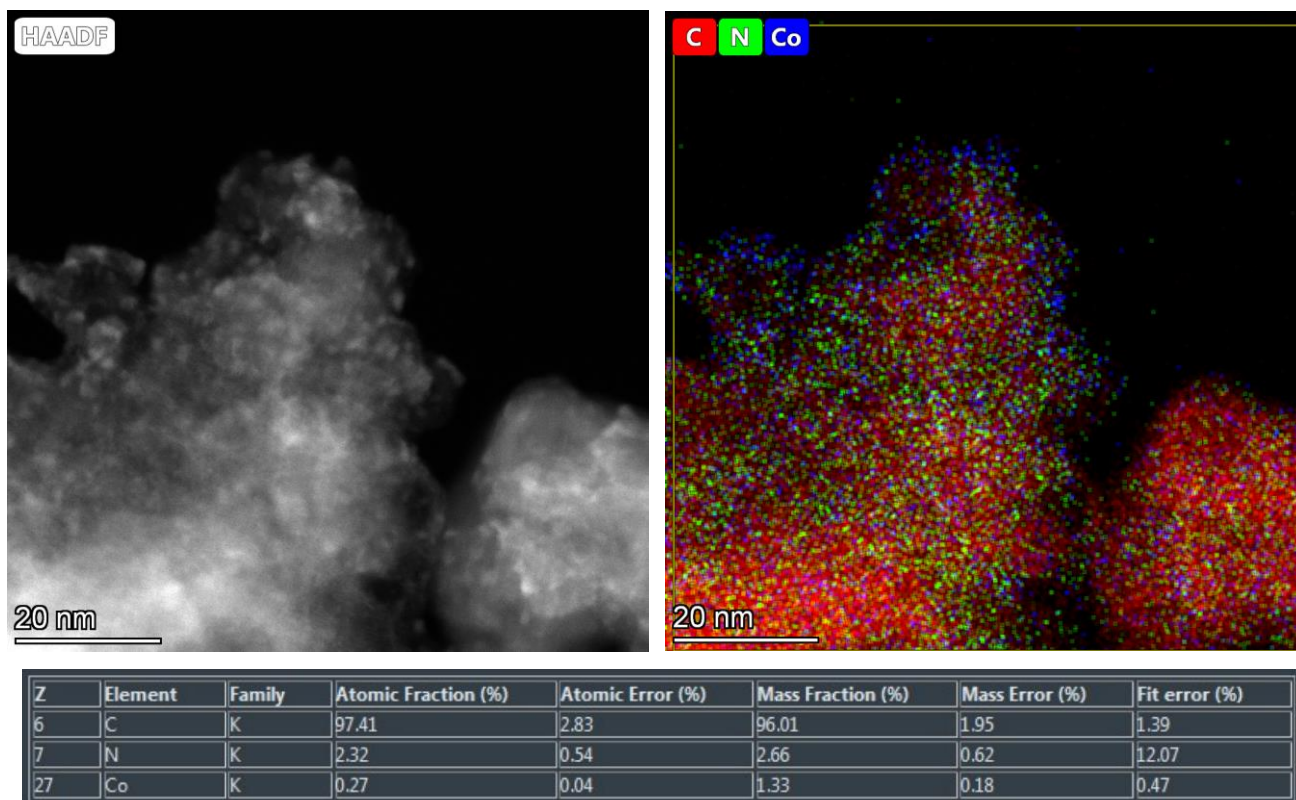
Fig. S1. TEM images of Co@NC-Gr.

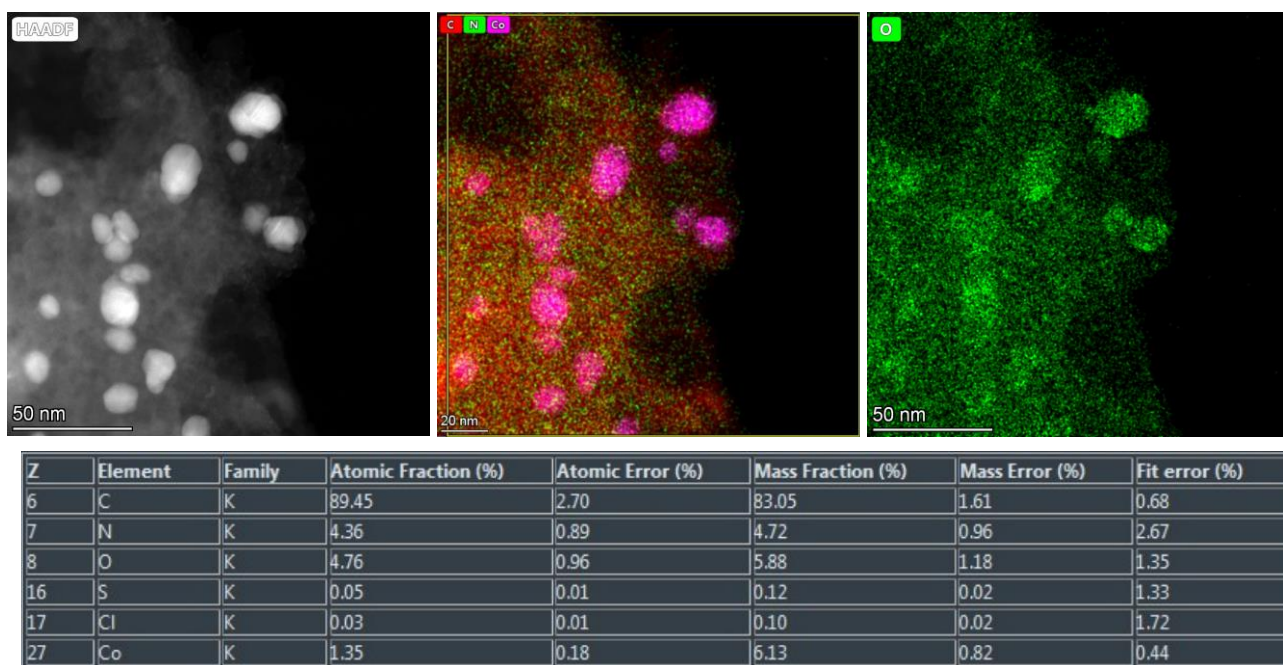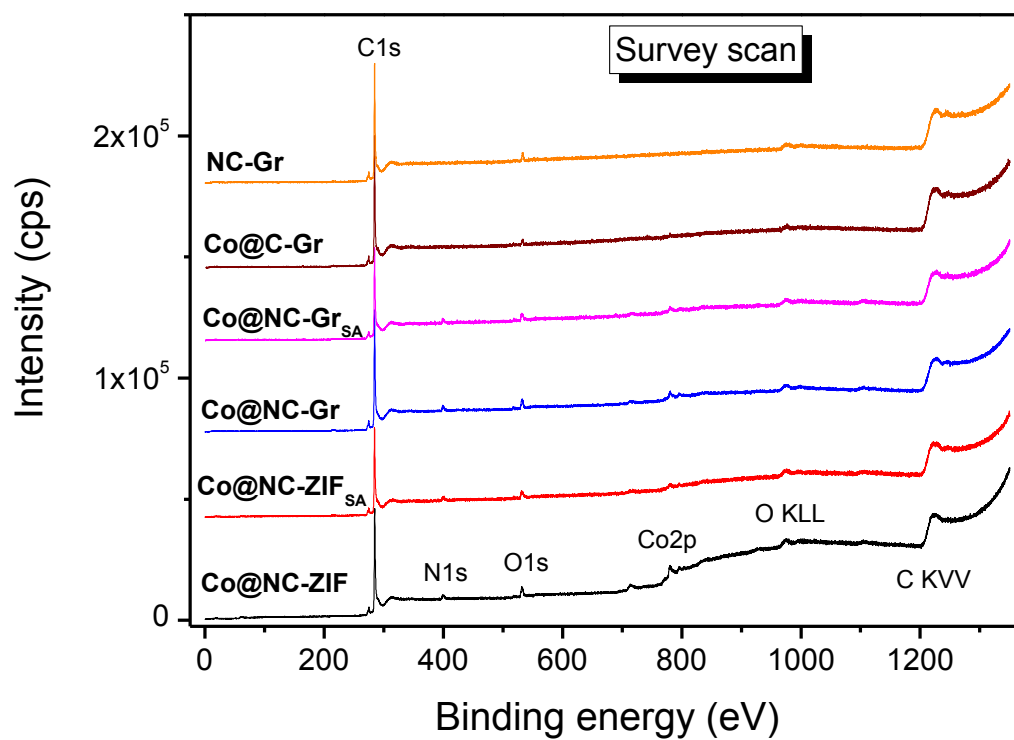**Fig. S2.** TEM images and EDX analysis of Co@NC-ZIF.

Fig. S3. (a) EDX-STEM mixed Co/C mapping image and (b-d) TEM images of Co@NC-Gr$_{SA}$.

Z	Element	Family	Atomic Fraction (%)	Atomic Error (%)	Mass Fraction (%)	Mass Error (%)	Fit error (%)
6	C	K	97.41	2.83	96.01	1.95	1.39
7	N	K	2.32	0.54	2.66	0.62	12.07
27	Co	K	0.27	0.04	1.33	0.18	0.47

Fig. S4. HAADF and EDX-STEM mixed C/N/Co mapping images of Co@NC-ZIF$_{SA}$ with atomic and mass fraction analysis.

Z	Element	Family	Atomic Fraction (%)	Atomic Error (%)	Mass Fraction (%)	Mass Error (%)	Fit error (%)
6	C	K	89.45	2.70	83.05	1.61	0.68
7	N	K	4.36	0.89	4.72	0.96	2.67
8	O	K	4.76	0.96	5.88	1.18	1.35
16	S	K	0.05	0.01	0.12	0.02	1.33
17	Cl	K	0.03	0.01	0.10	0.02	1.72
27	Co	K	1.35	0.18	6.13	0.82	0.44

Fig. S5. HAADF and EDX-STEM mixed C/N/Co and O mapping images of Co@NC-ZIF$_{SA}$ for the area containing Co/CoO$_x$ nanoparticles, with atomic and mass fraction analysis.

Fig. S6. Survey XPS of the samples.

Fig. S7. Conversions of ethanol under non-oxidative conditions as a function of temperature. Gas mixture: 5 vol.% EtOH, He balance; GHSV = 18000 h^{-1}.

Table S1. The XPS-derived chemical composition of the samples (%).

Sample	C	N	O	Co
Co@NC-ZIF	90.4	3.4	4.6	1.6
Co@NC-ZIF$_{SA}$	91.8	3.5	4.1	0.6
Co@NC-Gr	92.0	3.6	3.9	0.5
Co@NC-Gr$_{SA}$	91.3	3.7	4.4	0.6
Co@C-Gr	97.7	0.0	2.1	0.2
NC-Gr	96.0	0.5	3.5	0.0

Table S2. The XPS-derived atomic fractions of elements in the samples.

Sample	Co/N	Co/C	N/C
Co@NC-ZIF	0.48	0.018	0.04
Co@NC-ZIF$_{SA}$	0.18	0.007	0.04
Co@NC-Gr	0.15	0.006	0.04
Co@NC-Gr$_{SA}$	0.16	0.006	0.04
Co@C-Gr	-	0.002	0.00
NC-Gr	0.00	0.000	0.005

Table S3. The relative contribution of carbon species in the C 1s spectra (%).

Sample	C-C, C=C	C-N-C, C-O	C=O, COOH	CO_3^{2-}
Co@NC-ZIF	65.1	22.9	6.5	5.5
Co@NC-ZIF$_{SA}$	61.1	24.1	8.5	6.2
Co@NC-Gr	65.5	23.2	6.6	4.7
Co@NC-Gr$_{SA}$	62.0	27.4	6.2	4.4
Co@C-Gr	71.3	20.3	4.4	4.0
NC-Gr	69.5	22.5	4.3	3.8

Table S4. The relative contribution of nitrogen species in the N 1s spectra (%).

Sample	pyridinic-N	graphitic-N	NO_x
Co@NC-ZIF	45.5	35.7	18.8
Co@NC-ZIF$_{SA}$	44.6	38.7	16.7
Co@NC-Gr	58.4	28.6	13.0
Co@NC-Gr$_{SA}$	56.5	31.0	12.5
Co@C-Gr	_	_	_
NC-Gr	25.6	58.7	15.7

Table S5. Textural parameters of the samples.

Catalyst	S_{BET} (m^2 g^{-1})	V_{total} (cm^3 g^{-1})	$V_{micropore}$ (cm^3 g^{-1})	$V_{mesopore}$ (cm^3 g^{-1})	$S_{micropore}$ (m^2 g^{-1})	$S_{mesopore,}$ (m^2 g^{-1})
Co@NC-ZIF	174	0.35	0.01	0.34	27	147
Co@NC-ZIF$_{SA}$	507	0.36	0.24	0.12	456	51
Co@NC-Gr	93	0.24	0.03	0.21	71	22
Co@NC-Gr$_{SA}$	45	0.19	0.00	0.19	8	37
Co@C-Gr	234	0.72	0.03	0.69	66	168
NC-Gr	202	0.80	0.02	0.72	42	160
VulcanXC72R[a]	218	0.41	0.03	0.38	65	153

[a] I.J. Sanders, T.L. Peeten, Carbon Black: Production, Properties and Uses, Nova Science Publishers, London, 2011.